ResearchGate

See discussions, stats, and author profiles for this publication at: https://www.researchgate.net/publication/327237171

Photoluminescent Properties of Eu3+ Doped TiO2 Nanoparticles Synthesized Using an Acid Sulfuric Method

Article *in* Wulfenia · August 2018

CITATIONS
0

READS
46

7 authors, including:

Nguyen Trung Duong
Hue University - Quang Tri Campus
7 PUBLICATIONS **10** CITATIONS
SEE PROFILE

Dang Anh Tuan
Ha Nam Department of Science and Technology, Vietnam
15 PUBLICATIONS **23** CITATIONS
SEE PROFILE

Son Nguyen Manh
Hue University
12 PUBLICATIONS **42** CITATIONS
SEE PROFILE

Vo Thanh Tung
Hue College of Sciences, Hue Univercity, Vietnam
20 PUBLICATIONS **32** CITATIONS
SEE PROFILE

Some of the authors of this publication are also working on these related projects:

Preparation and study of optical properties of rare earth ionic doped nano-TiO2 View project

All content following this page was uploaded by Nguyen Trung Duong on 31 August 2018.

The user has requested enhancement of the downloaded file.

Photoluminescent Properties of Eu^{3+} Doped TiO_2 Nanoparticles Synthesized Using an Acid Sulfuric Method

Nguyen Trung Duong (Corresponding author)
Hue University – Quang Tri campus, Vietnam
College of Sciences, Hue University, Vietnam;
Tel: +84-914-612797 E-mail: nguyentrungduongps@gmail.com
Dang Anh Tuan
Ha Nam Department of Science and Technology, Vietnam;
Tel: +84-954-954966 E-mail: danganhtuan.khcn@hanam.gov.vn
Nguyen Manh Son
College of Sciences, Hue University, Vietnam;
Tel: +84-905-137823 E-mail: manhson03@yahoo.com
Vo Thanh Tung
College of Sciences, Hue University, Vietnam;
Tel: +84-935-961369 E-mail: votungbeo@gmail.com
Ho Van Tuyen
Duy Tan University, Vietnam;
Tel: +84-972-026929 E-mail: hovantuyen@gmail.com
Le Dai Vuong
Hue Industrial College, Vietnam;
Tel: +84-888-000858 E-mail: ledaivuongqb@gmail.com
Truong Van Chuong
College of Sciences, Hue University, Vietnam;
Tel: +84-914-089703 E-mail: truongvanchuong@yahoo.com

Abstract

In this paper, the structure and optical properties of Eu^{3+}-doped TiO_2 nanoparticles were studied. The results obtained by X-ray diffractometer patterns confirmed that the doping of Eu^{3+} ions into a nanostructured TiO_2 substrate prevents the crystalline formation and delays the variation of the phase structure as compared with the pure TiO_2 nanoparticles. The optical measurements showed that Eu^{3+} ions located on the surface of an amorphous TiO_2 matrix cause the photoluminescence phenomenon.

Keyword: TiO_2, europium, nanoparticles, ultrasound

1. Introduction

TiO_2 has wide applications in various fields such as photocatalytic [1–3, 15], solar cells [4–9], and split water into hydrogen fuel [10–13]. TiO_2 primarily exists in the following three forms: anatase, rutile, and brookite. TiO_2 has a large bandgap of about 3.2 eV, so it is easy for doping rare-earth ions. Recently, TiO_2 has been considered as a new substrate for radiations in the visible-infrared region.

The doping of a few rare-earth ions into the TiO_2 nanoparticle host has been carried out by several methods such as sol-gel method [14–21], hydrothermal method [22, 23], and other methods [24,25]. These methods are considered to be highly complex with high-cost precursors. In this paper, a simple and cheap process was used to prepare Eu^{3+}-doped TiO_2 nanoparticles. The influence of doping concentration and calcination temperature on the optical properties and structure phases of Eu^{3+}-doped TiO_2 nanoparticles was also observed.

2. Experimental Procedures

2.1. Chemicals

Commercial titanium dioxide powder TiO_2 (Merck), sulfuric acid H_2SO_4 (98%), $NH_4(OH)$ solution, and $Eu(NO_3)_3$ were used as starting materials. In addition, distilled water was used as a medium.

2.2. Characterizations

X-ray diffractometer (XRD, Cu Kα: α = 1.542 Å, D8 Advance, BRUKER–AXS) was used for identifying the phase structure in the as-prepared samples. The anatase volume fraction, X_A, and the average grain size, D, were, respectively, calculated by using the following equations [26,27]:

$$X_A(\%) = \frac{I_A}{I_A + 1.265 I_R} \times 100, \quad (1)$$

$$D = \frac{K\lambda}{\beta \cos\theta'} \quad (2)$$

where $I_{A/R}$ is the corresponding anatase (A) and rutile (R) peak intensities, D is the particle size, λ (= 0.15406 nm) is the wavelength of the used X-ray radiation, Kisa constant taken as 0.9, θ is the diffraction angle, and β is the full width at half-maximum of the corresponding XRD peak. In this case, the (101) and (110) diffraction peaks were used for anatase and rutile structures, respectively.

Scanning electron microscopy (SEM, Nova nanoSEM 450-FEI) and transmission electron microscopy (TEM, JEOL JEM–4000EX, 400 kV) were used to analyze the morphologies of the investigated materials.

A Raman spectrometer (Jobin-Yvon Inc., Paris, France) at a backscattering configuration was used to measure Raman scattering spectra. The excitation laser was emitted from an argon ion (Ar^+) laser source with a wavelength of 488 nm and a San output power of 11 mW. A spectrophotometer (FL3–22 HORIBA) with double monochromators was used to record the photoluminescence (PL) emission and excitation spectra.

2.3. Synthesis of nanosized TiO_2

In our previous work [28], the preparation of nanostructured TiO_2 particles was reported. The commercial TiO_2 powder was dispersed in the H2SO4 solution by using an ultrasonic device. Thereafter, the composition was added to distilled water and heated at 100°C for 1 h. The pH of the

compound was adjusted to 8 by adding the $NH_4(OH)$ solution. The white precipitates were filtered and washed many times by distilled water and then treated at various temperatures for 2 h. As illustrated in Figure 1, the morphology of the final product showed that the obtained particles are spherical in shape with their diameter in nanoscale.

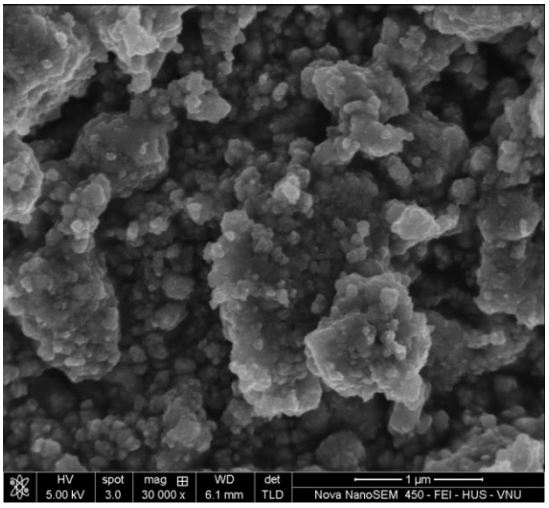

Figure 1. SEM image of TiO_2 nanoparticles after annealing at 450°C for 2 h

2.4. Synthesis of Eu^{3+}-doped TiO_2 samples

Eu^{3+}-doped TiO_2 samples were denoted by TiO_2:Eu*X* (where *X* is the content of Eu^{3+} ions in %mol, *X* = 0, 1, 2, 4, 8, 12, and 15). TiO_2 nanostructured powder and $Eu(NO_3)_3$ are required to be converted into a solution form in order to synthesize TiO_2:Eu*X* samples.

First, 0.5 g nanostructured TiO_2 powder was dissolved in the mixture of 20 mL H_2O_2 and 10 mL $NH_4(OH)$ to obtain a yellow transparent solution. Figure 2 shows the TEM image of the TiO_2 solution.

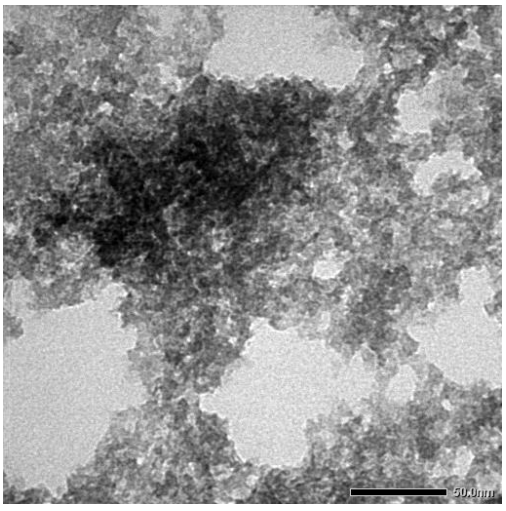

Figure 2. TEM image of TiO_2 nanosolution

Second, the 0.01M $Eu(NO_3)_3$ solution was added to TiO_2 nanosolution with different concentrations and then the solution was magnetically stirred at 100°C for 2 h. The obtained powder was annealed at different temperatures for 2 h.

3. Results and Discussion

3.1. The structure and microstructure of the pure TiO_2 and Eu^{3+}-doped TiO_2

XRD patterns of TiO_2:Eu0 and TiO_2:Eu4 powders calcined at different temperatures are presented in Figure 3. The percentages of the anatase phase, X_A, and the average grain size, D, were calculated and presented in Table 1. It can be seen that the effect of the calcination temperature on the phase structure is the same in the manner for two materials. As the temperature increases, the variation in structure undergoes through amorphousness, anatase, and rutile phases. However, there is a slight difference in the phase component at each calcination temperature. The pure TiO_2 powder has exhibited anatase structure at 450 °C, whereas TiO_2:Eu4 possesses an amorphous phase at this temperature. The existence of anatase and rutile phases in the TiO_2:Eu0 powder was observed at 650 °C, whereas the anatase phase was completely occupied in the TiO_2:Eu4 materials. The anatase-rutile transition did not appear until the temperature was 750°C for the TiO_2:Eu4 sample. TiO_2:Eu0 exhibited the rutile phase structure at an annealing temperature of 950 °C, whereas TiO_2:Eu4 remained as a part of the anatase phase with 19.6%. Finally, it can be concluded that the doping of Eu^{3+} ions into a nanostructure TiO_2 substrate prevented the crystalline formation and delayed the variation of the phase structure as compared with the pure TiO_2 nanoparticles.

As shown in Table 1 and Figure 4, the grain sizes of the pure TiO_2 and doped TiO_2 powders was increased as the calcination temperature increased. Especially, the grain size of the pure TiO_2 samples was larger than that of the doped TiO_2 specimens for each annealing temperature. Therefore, it can be concluded that the doping of Eu^{3+} ions into TiO_2 nanoparticles can repress the revolution of the grain size in materials.

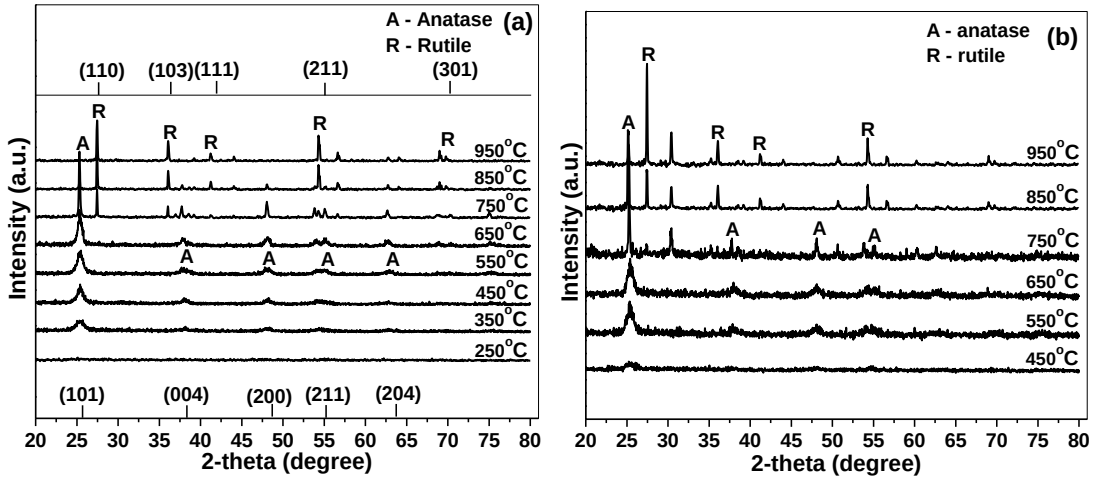

Figure 3. XRD patterns of TiO_2:Eu0 (a), and TiO_2:Eu4 nanoparticles (b) annealed at 350°C to 950°C.

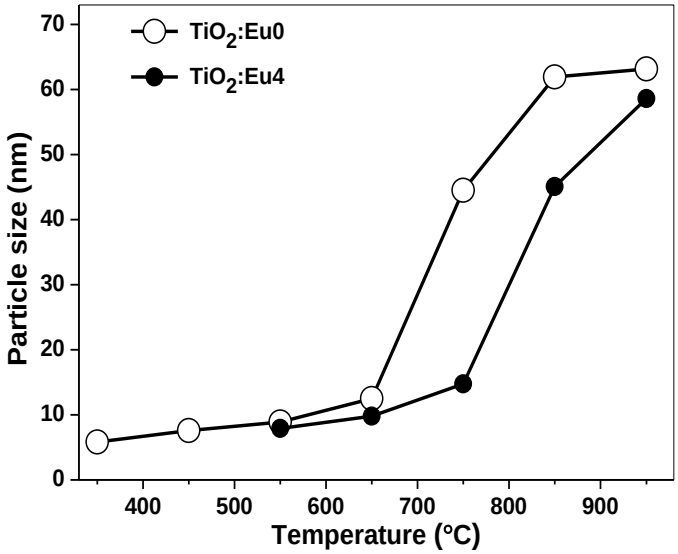

Figure 4. Particle size as a function of calcinating temperature for TiO_2:Eu0 and TiO_2:Eu4 materials

Table 1. The fraction of anatase phase (X_A) and the estimated average particle size for TiO_2:Eu0 and TiO_2:4Eu nanoparticles at different temperatures

Temperature (°C)	D (nm)		X_A (%)	
	TiO_2:Eu0	TiO_2:Eu4	TiO_2:Eu0	TiO_2:Eu4
350	5.8	-	100	-
450	7.6	-	100	-
550	8.9	7.9	*100*	*100*
650	12.5	9.81	94.9	100
750	44.5	14.75	70.6	91.91
850	61.92	45.08	37.5	72.13
950	63.15	58.61	1.3	19.61

The Raman spectra of TiO_2:Eu0 and TiO_2:Eu4 samples treated at various temperatures were measured and illustrated in Figure 5. The Raman bands characterized for anatase (392, 510, and 633 cm−1) and rutile phases (440 and 610 cm^{-1}) were clearly seen [18, 29, 30]. This result is in a complete agreement with the above-described XRD analysis. The Raman spectra of the Eu^{3+}-doped TiO_2 specimen are quite similar to those of the pure TiO2 specimen except for a slight shift as a result of impurity doping [13, 18, 23, 25].

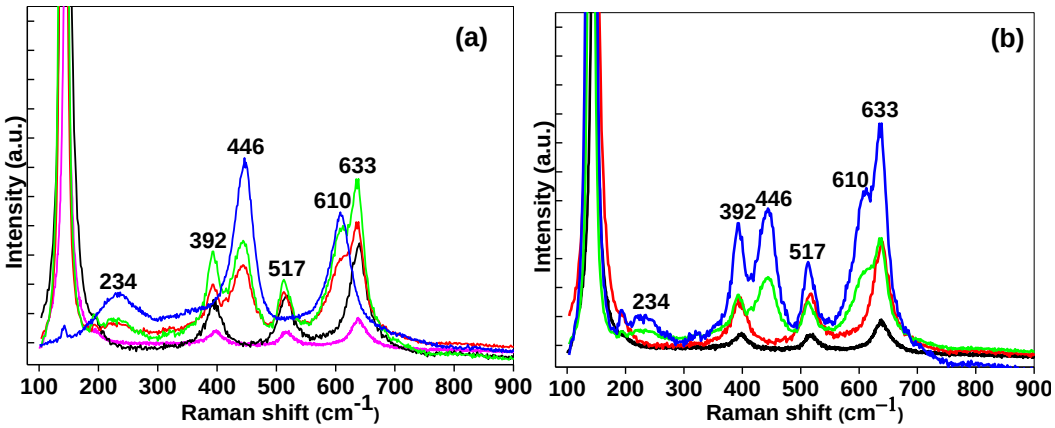

Figure. 5. Raman spectra of TiO_2:Eu0 (a) and TiO_2:Eu4 (b) nanoparticles at room temperature

3.2. The optical properties of Eu^{3+}-doped TiO_2

We measured excitation and emission spectra by using luminescence spectroscopy in order to study the optical properties. Figure 6 presents the excitation spectra of TiO_2:Eu4 samples annealed at 350°C to 950°C at an emission wavelength of 615 nm. Obviously, it can be observed that 362, 383, 394, 415, 464, 525, and 532 nm peaks are attributed to excitation transitions from the ground states to the excited states as $^7F_0 \rightarrow {}^5D_4$, $^7F_0 \rightarrow {}^5L_7$, $^7F_0 \rightarrow {}^5L_6$, $^7F_0 \rightarrow {}^5D_3$, $^7F_0 \rightarrow {}^5D_2$, $^7F_0 \rightarrow {}^5D_1$, and $^7F_1 \rightarrow {}^5D_1$, respectively [31–34]. Among them, the peaks at 393 nm and 464 nm seem to be the strongest for all samples.

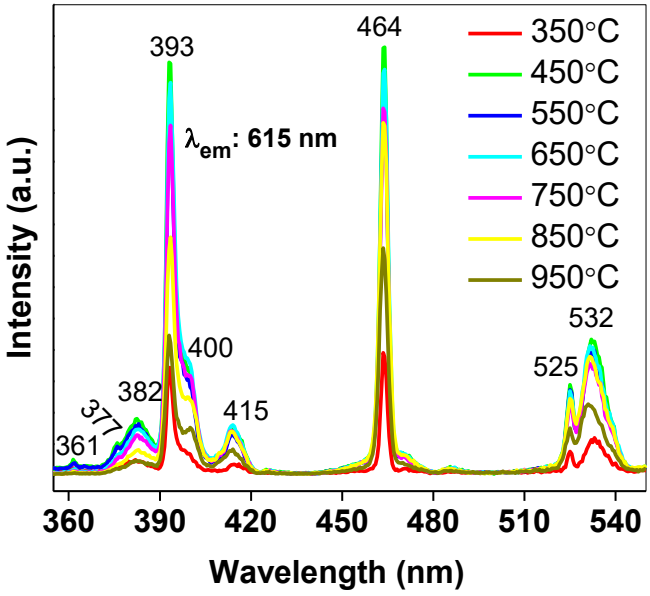

Figure 6. Photoluminescence excitation spectra of TiO_2:Eu4 sample annealed at differenttemperatures

Figure 7 shows the PL spectra of TiO_2:Eu4 specimens at room temperature treated at different temperatures under the 393 nm excitation.

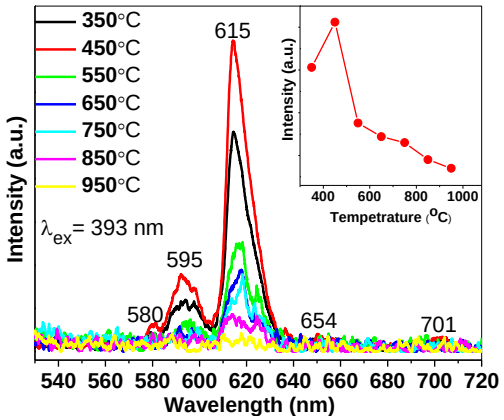

Figure 7. Photoluminescence emission spectra of TiO_2:Eu4 nanoparticles

It can be clearly seen that the PL curves possess five emission bands corresponding to the transitions from the excited states to the ground states of Eu^{3+} ions. These peaks are centered at 580, 595, 615, 654, and 701 nm and assigned to emission transitions of $^5D_0$–^7F_j (j = 0–4), respectively [32,33]. From the inset of Figure 7, it can be observed that the PL intensity increased as the annealing temperature was less than or equal to 450°C with the material possessing an amorphous phase. Beyond a temperature of 450°C, the amplitude of the PL peak decreased monotonically. The luminescence phenomenon was not even observed as the calcination temperature increased beyond 950°C. It was believed that the Eu^{3+}-doped amorphous TiO_2 matrix could better affect the received PL phenomenon as compared with the crystalline form.

Figure 8 shows the PL emission spectra of TiO_2:Eu*X* samples annealed at 450°C for 2 h. As shown in the Figure, the concentration of Eu^{3+} strongly affected the PL characterization. With the increasing Eu^{3+} addition in the range of 1–15 mol%, the PL intensity continuously increased (see the inset of Figure 8). In this study, the concentration quenching phenomenon is not analyzed. Considering the ion radii of 0.0946 and 0.074 nm for Eu^{3+} and Ti^{4+}, respectively, Eu^{3+} ions would not substitute for Ti^{4+} within TiO_2, so Eu^{3+} ions could only be located on the surface of the TiO_2 matrix that causes the PL emission phenomenon.

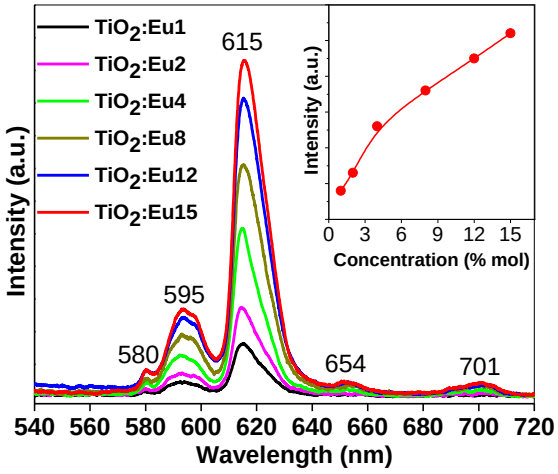

Figure 8. Photoluminescence emission Spectra of TiO_2:Eu*X* samples annealed at 450°C for 2 h

4. Conclusion

We have successfully synthesized Eu^{3+}-doped TiO_2 nanoparticles with an acid sulfuric method by using an ultrasonic device. The obtained results confirmed that the structure and optical properties are strongly affected by doping concentration and calcination *temperature*. Consequently, the maximum PL intensity was obtained for the TiO_2:Eu4 sample calcinated at 450°C and it continuously increased with the increase in the content of the dopant (Eu^{3+}).

Acknowledgements

The study was financed by the scientific research projects of Hue University under Number DHH2016-13-02

References

[1]. Reszczynska, J., Iwulska, A., Sliwinski, G., Zaleska, A. (2012). Characterization and photocatalytic activity of rare earth metal – doped Titanium Dioxide. *Physicochemical Problems of Mineral Processing*, 48(1), 201 – 208

[2]. Hashimoto, K., Irie, H. and Fujishima A. (2005). TiO_2 photocatalysis a historical overview and future prospect. *Japanese Journal of Applied Physics*, 44(12), 8269-8285

[3]. Nakata, K., Fujishima, A. (2012). TiO_2 photocatalysis Design and applications.*Journal of Photochemistry and Photobiology C: Photochemistry Reviews*,13, 169– 189

[4]. Chi-Hwan, H., Hak-Soo, L., Kyung-won, L., Sang-Do, H., and Singh, I. (2009). Synthesis of Amorphous Er^{3+}-Yb^{3+} Co-doped TiO_2 and Its Application as a Scattering Layer for Dye-sensitized Solar Cells. *Bulletin of the Korean Chemical Society*, 30(1), 219

[5]. Dui Yanto Rahman, Mamat Rokhmat, Elfi Yuliza, Euis Sustini, Mikrajuddin Abdullah (2016). New design of potentially low-cost solar cells using TiO_2/graphitecomposite as photon absorber. *International Journal of Energy and Environmental Engineering*

[6]. Bach, U., Lupo, D., Comte, P., Moser, J. E., Weissortel, F., Salbeck, J., Spreitzer, H., Gratzel, M. (1998). Solid-state dye-sensitizedmesoporous TiO_2 solar cells with high photon-to-electronconversion efficiencies. *Letters to Nature*, 395

[7]. Mor, G. K., Shankar, K., Paulose, M., Varghese, O. K., and Grimes, C. A. (2006). Use of Highly-Ordered TiO_2 Nanotube Arrays in Dye-Sensitized Solar Cells. *Nano Letters*, 6(2), 215-218

[8]. Robel, I., Subramanian, V., Kuno, M., and Kamat, P. V. (2006). Quantum Dot Solar Cells. Harvesting Light Energy with CdSeNanocrystals Molecularly Linked to Mesoscopic TiO_2 Films. *Journal of the American Chemical Society*, 128, 2385-2393

[9]. Roose, B., Pathak, S., and Steiner, U. (2015). Doping of TiO_2 for sensitized solar cells. *Royal Society of Chemistry*

[10]. Ismail, A. A., Bahnemann, D. W. (2014). Photochemical splitting of water for hydrogen production by photocatalysis: A review. *Solar Energy Materials & Solar Cells*, 128, 85 – 101

[11]. Selli, E., Chiarello, G. L. , Quartarone, E., Mustarelli, P., Rossetti, I., and Forni, L. (2007). A photocatalytic water splitting device for separate hydrogen and oxygen evolution, *Chemical Communications*, 5022–5024

[12]. Chowdhury, P., Malekshoar, G. and Ray, A. K. (2017). Dye-Sensitized Photocatalytic Water Splitting and Sacrificial Hydrogen Generation: Current Status and Future Prospects. *Inorganics*, 5, 34,

[13]. Xie, M.-Y., Su, K.-Y., Peng, X.-Y., Wu, R.-J., Chavali, M., Chang, W.-C. (2016). Hydrogen production by photocatalytic water-splitting on Pt-doped TiO_2–ZnO under visible light. *Journal of the Taiwan Institute of Chemical Engineers, 1–7*

[14]. Devi, R. S., Venckatesh, R., Sivaraj, R. (2014). Synthesis of Titanium Dioxide Nanoparticles by Sol-Gel Technique. *International Journal of Innovative Research in Science, Engineering and Technology*, 3

[15]. Karami, P. A. (2010). Synthesis of TiO_2 nano powder by the sol-gel method and its use as a photocatalyst. *Journal of the Iranian Chemical Society*, 7, S154-S160

[16]. Devi, R. S., Venckatesh, R., Sivaraj, R. (2014). Synthesis of Titanium Dioxide Nanoparticles by Sol-Gel Technique. *International Journal of Innovative Research in Science Engineering and Technology*, 3

[17]. Borlaf, M. , Wu, H.-M., Colomer, M. T. , Moreno, R. , and Tseng, W. J. (2012). Synthesis and Characterization of Anatase-Structured Titania Hollow Spheres Doped with Erbium (III). *Journal of the American Ceramic Society*, 95(9), 3005–3011

[18]. Cao, Y., Zhao, Z., Yi, J., Ma, C., Zhou, D., Wang, R., Li, C., Qiu, J. (2013). Luminescence properties of Sm^{3+}-doped TiO_2 nanoparticles: Synthesis, characterization, and mechanism. *Journal of Alloys and Compounds*, 554, 12–20

[19]. Shang, Q., Yu, H., Kong,X., Wang, H., Wang, X., Sun, Y., Zhang, Y., Zeng, Q., (2008). Green and red up-conversion emissions of Er^{3+}–Yb^{3+} Co-doped TiO_2 nanocrystals prepared by sol–gel method. *Journal of Luminescence*, 128, 1211–1216

[20]. Zhang, I., Wang, X., Zheng, W.-T., Kong, X.-G., Sun, Y.-J., Wang, X. (2007). Structure and luminescence properties of TiO2:Er^{3+} nanocrystals annealed at different temperatures. *Material Letters*, 61, 1658-1661

[21]. Luo, M., Cheng, K., Weng, W., Song, C., Du, P., Shen, G., Xu, G., Han, G. (2009). Enhanced Luminescence of Eu-Doped TiO_2 Nanodots. *Nanoscale Research Letters* , 4, 809–813

[22]. Hsiao–Yen Lee and Girish M. Kale (2008). Hydrothermal Synthesis and haracterization of Nano-TiO_2.*American Ceramic Society*, Vol. 5, No. 6

[23]. Zhenquan Tan, Kazuyoshi Sato, Satoshi Ohara (2014). Synthesis of layered nanostructured TiO_2 by hydrothermal method.*Advanced Powder Technology*

[24]. Chander, H. (2006). A Review on Synthesis of Nanophosphors – Future Luminescent Materials. *Proceeding. of ASID.*

[25]. Vijayalakshmi, R. and Rajendran, V. (2012). Synthesis and characterization of nano-TiO_2 via different methods. *Archives of Applied Science Research*, 4 (2), 1183-1190

[26]. Su, R., Bechstein, R., So, L., Vang, R. T., Sillassen, M., Esbjornsson, B., Palmqvist, A. and Besenbacher, F. (2011). How the Anatase-to-Rutile Ratio Influences the Photoreactivity of TiO_2. *Journal of Physical Chemistry*, 115, 24287–24292

[27]. Azizi, K. F., Mohagheghi, B. (2013). Transition from anatase to rutile phase in titanium dioxide (TiO_2) nanoparticles synthesized by complexing sol–gel process: effect of kind of complexing agent and calcinating temperature. *Journal of Sol-Gel Science and Technology*, 65, 329–335

[28]. Duong, N. T., Vuong, L. D., Son, N. M., Tuyen, H. V. and Chuong, T. V. (2017). The synthesis of TiO_2 nanoparticles using sulfuric acid method with the aid of ultrasound. *Nanomaterials and Energy*, 6(2), 82-88

[29]. Choi, H. C., Jung, Y. M., Kim, S. B. (2005). Size effects in the Raman spectra of TiO_2 nanoparticles. *Vibrational Spectroscopy*, 37, 33–38

[30]. Mazza, T., Barborini, E., Piseri, P., and Milani, P. (2007). Raman spectroscopy characterization of TiO_2 rutile nanocrystals. *Physical Review B*, 75, 045416

[31]. Zhao, J., Duan, H., Ma, Z., Wang, T., Chen, C. and Xie, E. (2008). Temperature and TiO_2 content effects on the photoluminescence properties of Eu^{3+} doped TiO_2 – SiO_2 powders. *Journal of Applied Physics*, 104, 053515

[32]. Ratnakaram, Y. C., Prasad, V. R., Babu, S. and Kumar, V. V. R. K. (2016). Luminescence performance of Eu^{3+}-doped lead-free zinc phosphate glasses for red emission. *Bulletin of Materials Science*, 39(4), 1065–1072

[33]. Shwetha, M., Eraiah, B. (2018). Influence of europium (Eu^{3+}) ions on the optical properties of lithium zinc phosphate glasses. *IOP Conference Series: Materials Science and Engineering*, 310, 012033

[34]. Liu, H. and Yu, L. (2013). Preparation and Photoluminescence Properties of Europium Ions Doped TiO_2 Nanocrystals. *Journal of Nanoscience and Nanotechnology*, 13, 5119–5125

View publication stats